JOURNAL OF COMPUTATIONAL PHYSICS **44**, 220–226 (1981)

Note

Conformal Mappings for Internal Viscous Flow Problems

Isolated occlusions in a straight channel or pipe can be described analytically in a fashion that allows efficient, accurate computation of nonlinear flow fields through conformal transformations.

INTRODUCTION

Many incompressible viscous flow problems are approached theoretically via numerical simulation because the governing Navier–Stokes equation is nonlinear. For curved two-dimensional flow boundaries that do not correspond to well-known orthogonal curvilinear coordinate systems, it is often convenient to transform the problem to another rectangular computation plane via a one-to-one mapping [1–12]. Analytic conformal mappings have been relatively rare because in general the relevant mapping expression is unknown. However, the advantages of such transformations suggest seeking appropriate analytic formulas to match the given boundaries.

Our experience with such mapping functions for internal viscous flow problems has been very good [10, 11], as has been found for external boundary layer problems by Ghia and Davis [12]. Our interest in internal flow problems is due to the disease atherosclerosis, in which arteries are occluded by the growth of atheromatous plaque, often to the point of complete closure. To find the role of fluid mechanics in the continual development of the plaque, we were led to the idealized model of a single smooth axisymmetric occlusion in a long straight pipe. It was necessary to characterize the wall boundary, i.e., the "stenosis" shape, in order to calculate the corresponding periodic flow field. We sought simple conformal mappings (some described below), to define the shape in a realistic fashion that provided a convenient range of shape variations. The computed flow fields are described elsewhere, but the technique was so successful it is urged for other internal flow problems.

A brief discussion presents advantages of a conformal mapping technique followed by a list of disadvantages of other mappings. It describes a comparison study of steady flow solutions for a particular stenosis shape and fixed flow Reynolds number, which illustrates the preceding sections.

0021-9991/81/110220–07$02.00/0

ARTERIAL OCCLUSIONS

1. *Mapping the Boundary*

Our internal problem geometry was an isolated symmetric occlusion (narrowing) in a straight channel (or tube, in the axisymmetric version). The most obvious parameters of the occlusion are its relative depth δ (often expressed as throat ratio d_R) and its relative half-width λ (point from the throat where the local discrepancy is half the total). A satisfactory two-parameter conformal mapping is

$$\zeta = u + iv = Az + B \tanh \frac{\pi}{2} z, \qquad z = x + iy \text{ (or } x + ir); \tag{1}$$

$$u = Ax + B \sin \pi x (\cosh \pi x + \cos \pi y)^{-1},$$

$$v = Ay + B \sin \pi y (\cosh \pi x + \cos \pi y)^{-1}.$$

This yields a double family with wall boundary $y(x) = v_j$ [or $r(x)$ for axisymmetry] with choice of B/A. Figure 1 shows a map for Eq. (1) with fixed A, B from the uniform computational mesh; any curve corresponding to $v = v_j$ can be used as a boundary contour. There are automatically more points in the throat region just where they are desired. Figure 2 illustrates the half-width variation for fixed throat ratio = 0.5 as a function of v_j/A. Using this and similar graphs at other throat ratios we can get the correct coefficients of the conformal mapping of Eq. (1) to match the depth and half-width of the actual arterial stenosis artificially induced in a dog as part of our research project. This mapping function represents a portion of uniform inviscid flow through a screen of doublets placed in equidistant array normal to the flow.

Another double continuum of occlusion shapes sharper at the throat is given by

$$\zeta = Az + B \frac{\sinh(\pi/2)\, z}{\cosh^2(\pi/2)\, z} \tag{2}$$

for different screen singularities from Eq. (1). It is possible to get other occlusion shapes from the higher-order singularities obtained by differentiating the "disturbance

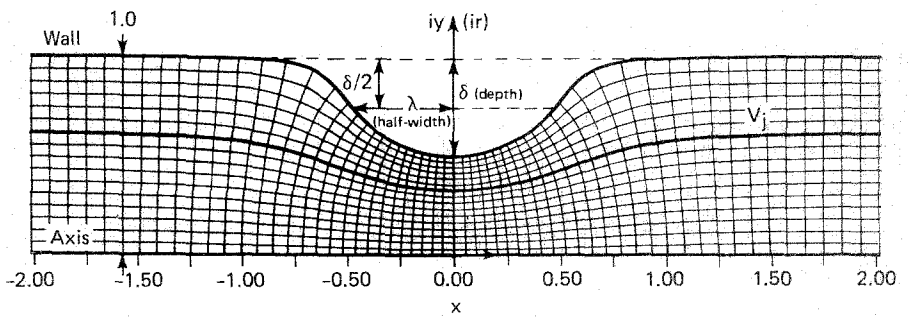

FIG. 1. Coordinate mesh for conformal stenoses, Eq. (1).

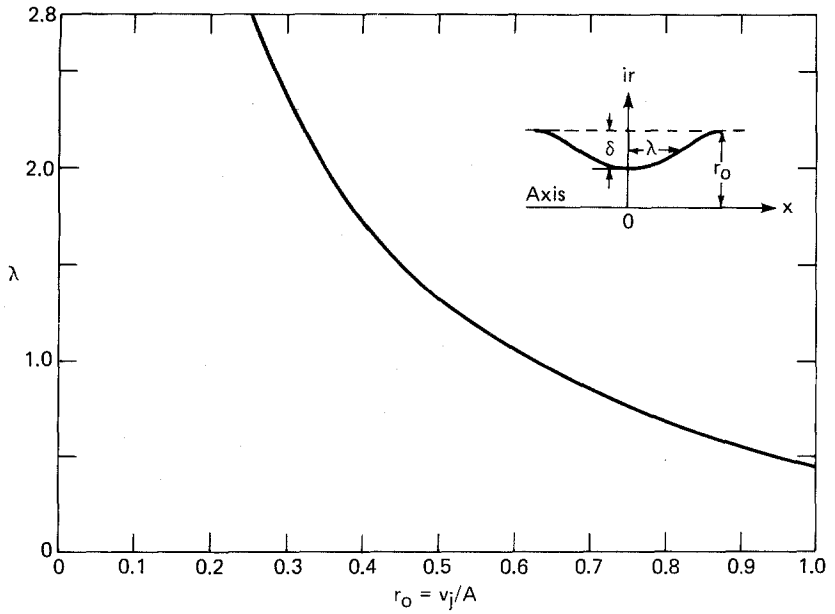

FIG. 2. Variation of relative half-width for a fixed throat ratio (0.50) with Eq. (1) mapping function.

function," the second term in Eq. (1) or (2). The occlusion shapes given by Eqs. (1) and (2) have fore-and-aft symmetry but a mapping with a single function without that property is given by

$$\zeta = Az - B \operatorname{sech}^2 \frac{\pi}{2} z, \tag{3}$$

which is illustrated in Fig. 3. This might represent an atherosclerotic occlusion followed by an aneurysm (post-stenotic dilatation). Other more complicated disturbance expressions that have the right behavior at $x = \pm\infty$ were also found. Because the conformal mapping function is linear, a number of analytic disturbance functions can be superposed. This suggests matching to a given occlusion shape in a least-squares sense by fitting coefficients to a singularity series, if closer matching is desired. If there is more than one occlusion, the singularity disturbance functions can be distributed at their locations. For instance, two equal narrowings located $(2a)$ apart can be imaged from

$$\zeta = Az + B \tanh \frac{\pi}{2}(z + a) + B \tanh \frac{\pi}{2}(z - a) \qquad \text{(a real)}. \tag{4}$$

There is no limit to the array of wall shapes that can be represented analytically and that allow conformal transformations of the corresponding internal flow fields.

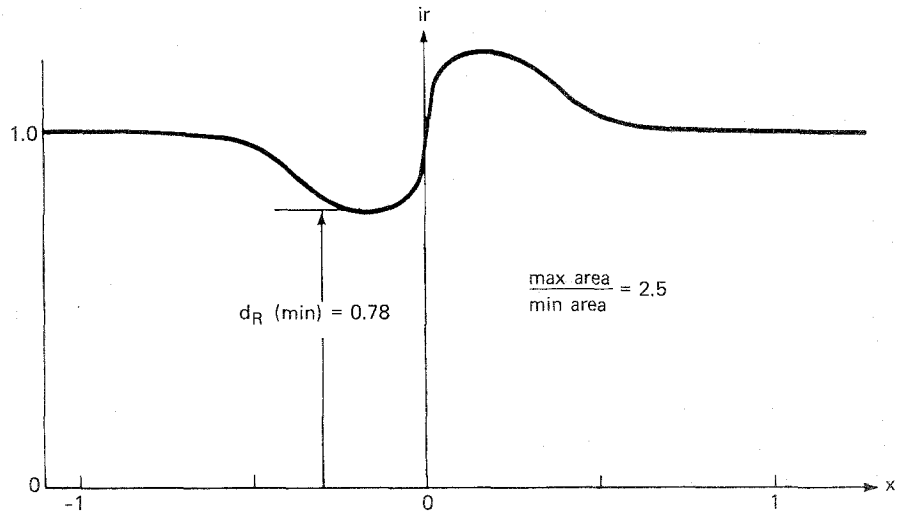

FIG. 3. Asymmetric wall shape for a constricted tube with mapping function, Eq. (3).

2. *Flow Equations*

Assuming a Newtonian incompressible fluid, the unsteady axisymmetric Navier–Stokes equation can be reduced to two coupled equations in Stokes stream-function ψ and vorticity magnitude Ω:

$$\Omega = -\frac{1}{r} D\psi, \tag{5a}$$

$$f_R \frac{\partial \Omega}{\partial \tau} + \frac{1}{2} \frac{\overline{Re}}{r} \left(J(\psi, \Omega) + \frac{\Omega}{r} \frac{\partial \psi}{\partial x} \right) = \frac{1}{r} D(r\Omega), \tag{5b}$$

where

$$D = \frac{\partial^2}{\partial r^2} - \frac{1}{r} \frac{\partial}{\partial r} + \frac{\partial^2}{\partial x^2}, \qquad J(\psi, \Omega) = \frac{\partial(\psi, \Omega)}{\partial(r, x)},$$

the reduced frequency $f_R = 2\pi r_0^2/(\nu T)$ and the inlet Reynolds number Re is $2Ur_0/\nu$. Here U is the space-average velocity in the inlet tube, r_0 is the inlet radius, ν is the kinematic viscosity of the fluid, T is the period of the pulsatile flow and $(\overline{Re})$ is the time mean. Nondimensional lengths r and x have been normalized by r_0 and $\tau = \omega t$ where $\omega = 2\pi/T$. The transformed equations corresponding to Eq. (1) are given in Ref. [13].

The assigned periodic waveform consists of a steady portion and a single harmonic $\cos \omega t$. The flow depends on amplitude ε where the normalized boundary stream-function (flux) is

$$\psi(\tau) = 1 + \varepsilon \cos \tau. \tag{6}$$

Viscous nonslip requires $\psi(\tau)$ constant along the solid wall and $\partial\psi/\partial n = 0$, where n is the normal. Parallel inflow and outflow that satisfy wall nonslip and Eqs. (5, 6) are specified as end conditions at locations far from the constriction.

3. *Solution*

The transformed vorticity equation (5b) was solved in finite-difference approximation by explicit Dufort–Frankel marching [13]. A time step was computed by determining Ω at the new time level, followed by solving the linear system (5a), then followed by computation of the wall vorticity to complete the time step. Usually Eq. (5a) is solved by a conjugate gradient technique, but other more efficient methods have also been developed. Convergence is checked after each cycle at the instant of maximum flux.

The computed pulsatile flow fields [10, 11] for moderately constricted arteries depend on three dynamic parameters (f_R, Re, ε) and will not be described here. A typical result is the cyclic behavior of the recirculation region that appears downstream of the throat.

Discussion

1. *Advantages of Analytic Conformal Mapping*

If the mapping is conformal it translates the normal and tangential velocity component boundary conditions in a natural way, generally allowing the viscous boundary condition to be met to the same order of approximation as the partial derivatives in the flow equation. The Laplacian operator (or any related second order elliptic operator) takes a simple form in the transformed plane without cross-derivative terms. Since all the mapping functional terms can be evaluated from analytic expressions there will be no errors introduced by the mapping. This does not mean that errors in the final approximate solution are not affected by the mapping, but if the transformed solution is exact, the mapping will not make it inexact. This seems to be reflected in no loss of numerical stability due to the mapping in time-dependent calculations. For arbitrarily shaped regions it is difficult to ascertain the "conformal module" to be matched in the mapped plane to ensure that physical corner points map correctly into the corner points of the computation plane [14], but this subtle constraint is automatically satisfied by the analytic expression [15–17].

2. *Disadvantage to Numerical Mappings*

There are many ways to do an approximate numerical mapping with or without conformality [1–9]. Nonconformal mappings sometime introduce trouble when the Jacobian goes to zero or even approaches it [5]. They also introduce cross-derivative terms into the transformed partial differential equations making them more cumbersome to program. So some workers have kept to conformal mappings [6–9]. However they introduce numerical errors because the mapped functions in the

transformed equation are approximate. This tends to reduce numerical stability. To improve the stability lower-order convective approximations (e.g., upwind differencing) are sometimes used to secure the nonlinear solution. This, of course, increases the error of the approximate solution, particularly when there is a local recirculation region, where reverse flow requires backward differencing. If a finer mesh or packed grid calculation is deemed necessary, the numerical transformation terms must be redone to the smaller scale.

3. *Comparison Studies*

By restricting the inflow to be steady, our method yielded the steady solution with a recirculation region just aft of the throat [13]. This same steady solution was also sought by a nonconformal numerical mapping but the system did not converge for the same time step, or even a much smaller one. The steady solution was obtained, however, by a direct iterative method with the numerical mapping and the results compared favorably. On the other hand, an implicit marching scheme with the numerical mapping appeared to converge satisfactorily, but to a wrong answer. The erroneous convergence limit was traced to a subtle mistake in setting the vorticity (viscous) boundary condition on the solid surface and was resolved [13].

The above comparison tests were carried out for an inlet Reynolds number Re based on diameter and mean velocity of 100 [$Re \equiv (2Ur_0/\nu)$]. Earlier numerical conformal mappings on similar occlusions had convergence limited to $Re \leqslant 25$ [6]. Another nonconformal mapping method showed significant discrepancies [5].

ACKNOWLEDGMENTS

This work was carried out with the financial support of the NIH under Grant HL23291. The programming efforts of L. W. Ehrlich and S. Favin are gratefully acknowledged.

REFERENCES

1. A. A. AMSDEN AND C. W. HIRT, *J. Comput. Phys.* **11** (1973), 348–359.
2. J. F. THOMPSON, F. C. THAMES, AND C. W. MASTIN, *J. Comput. Phys.* **15** (1974), 299–319.
3. J. F. THOMPSON, F. C. THAMES, C. W. MASTIN, AND S. P. SHANKS, *in* "Proceedings of the AIAA 2nd Computational Fluid Dynamics Conference, Hartford, Conn.," pp. 68–80, 1975.
4. F. C. THAMES, J. F. THOMPSON, C. W. MASTIN, AND R. L. WALKER, *J. Comput. Phys.* **24** (1977), 245–273.
5. W. L. OBERKAMPF AND S. C. GOH, *in* "Computational Mechanics," Lecture Notes in Mathematics, No. 461, pp. 569–580, Springer-Verlag, Berlin, 1974.
6. J. S. LEE AND Y. C. FUNG, *J. Appl. Mech.* **92** (1970), 9–16.
7. W. D. BARFIELD, *J. Comput. Phys.* **5** (1970), 23–33.
8. D. C. IVES, *AIAA J.* **14** (1976), 1006–1011.
9. S. B. POPE, *J. Comput. Phys.* **26**, (1978), 197–217.
10. V. O'BRIEN AND L. W. EHRLICH, *in* "Biofluid Mechanics" (D. J. Schneck, Ed.), Vol. 2, Plenum, New York, 1980.

11. V. O'BRIEN AND L. W. EHRLICH, *in* "Proceedings, 1977 Biomechanics Symposium" (R. Skalak and A. B. Schultz, Eds.), Vol. 23, p. 114, Amer. Soc. Mech. Engin., New York, 1977.
12. U. GHIA AND R. T. DAVIS, *AIAA J.* **12** (1974), 1659–1665.
13. L. W. EHRLICH, *Comput. Fluids* **7** (1979), 247–256.
14. C. D. MOBLEY AND R. J. STEWART, *J. Comput. Phys.* **34** (1980), 124–135.
15. N. E. KOCHIN, I. A. KIBEL, AND N. V. ROZE, "Theoretical Hydromechanics," Interscience, New York, 1964.
16. L. M. MILNE-THOMSON, "Theoretical Hydrodynamics," MacMillan, London, 1968.
17. P. HENRICI, "Applied and Computational Complex Analysis," Vol. 1, pp. 422–432, Wiley, New York, 1974.

RECEIVED: February 17, 1981; revised August 3, 1981

V. O'BRIEN

Milton S. Eisenhower Research Center
Applied Physics Laboratory
The Johns Hopkins University
Laurel, Maryland 20707

Printed in Belgium